# Template Polymerization to Fabricate Hydrogen-Bonded Poly(acrylic acid)/Poly(vinylpyrrolidone) Hollow Microcapsules with a pH-Mediated Swelling−Deswelling Property

Zhiqiang Feng, Zhipeng Wang, Changyou Gao,* and Jiacong Shen

*Key Laboratory of Macromolecule Synthesis and Functionalization, Ministry of Education, and Department of Polymer Science and Engineering, Zhejiang University, Hangzhou 310027, China*

*Received January 6, 2007. Revised Manuscript Received June 30, 2007*

Hydrogen-bonded hollow microcapsules with a lightly cross-linked shell structure were fabricated by polymerization of acrylic acid in a solution containing surface-modified silica particles and poly(vinylpyrrolidone) and a subsequent core removal with HF. By further incorporating additional cross-linkers, a highly cross-linked shell structure was produced, which endows the microcapsules with better stability against large pH fluctuations. The hollow and intact microcapsules in both wet and dry states were characterized and confirmed by TEM, SEM, AFM, and CLSM. The chemical compositions of the microcapsules and hydrogen bonding in the shells were determined by elemental analysis and FTIR spectroscopy, respectively. The continuous shells of the lightly cross-linked microcapsules on the silica particles are composed of PVP and PAA with an equal molar ratio of AA to VP. Alkaline treatment cannot separate PVP from PAA, which demonstrates the strong interactions between PAA and PVP. The lightly cross-linked and highly cross-linked microcapsules could increase their sizes along with the pH increase, following a sigmoidal regime. The capsule swelling−shrinking process is completely reversible at high and low pH values, respectively.

## Introduction

Hollow microcapsules with well-defined structures and tailorable properties have attracted more and more attention in recent years due to their potential applications in many fields such as medicine, drug delivery, artificial cells or viruses, and catalysis. For many potential applications, microcapsules environmentally sensitive to light, temperature, or pH are frequently required.[1,2] Structures held by hydrogen bonding are typically pH-sensitive systems.[3,4] For instance, the complexes of poly(acrylic acid) (PAA) and poly(vinylpyrrolidone) (PVP) remain stable at low pH values, whereas they dissociate above pH 5 due to abruption of the hydrogen bonding as a result of deprotonation of the PAA component.[5] Owing to this tunable feature, hydrogen bonding has been widely used as the driving force to fabricate smart capsules.[6] However, for practical applications, the structure of the hydrogen-bonded hollow capsules should be stabilized to avoid the discrete dissociation of the capsules at high pH.[7]

Thus far, many techniques have been developed to fabricate hollow microcapsules with variable features. Among the many techniques, cross-linking of shells of liposomes[8] or micellar diblock or triblock copolymer systems[9] is usually applied to producing stable hollow structures. This method has some advantages, such as the ease of fabrication of microcapsules with a sub-micrometer or nanometer size and narrow distribution. However, specific molecular structures are required to constitute the shells, and it is inconvenient to vary the capsule size. More recently, template-assisted polymerization on the surfaces of colloidal particles provides a new avenue to produce hollow capsules. By this technique, various methods, including emulsion polymerization,[10] miniemulsion polymerization,[11] dispersion polymerization,[1,12] and

* Corresponding author. E-mail: cygao@mail.hz.zj.cn; fax: +86-571-87951108.

(1) (a) Zha, L.; Zhang, Y.; Yang, W.; Fu, S. K. *Adv. Mater.* **2002**, *14*, 1090. (b) Sukhishvili, S. A. *Curr. Opin. Colloid Interface Sci.* **2005**, *10*, 37.
(2) (a) Angelatos, A. S.; Radt, B.; Caruso, F. *J. Phys. Chem. B* **2005**, *109*, 3071. (b) Zhang, Y.; Jiang, M.; Zhao, J.; Wang, Z.; Dou, H.; Chen, D. *Langmuir* **2005**, *21*, 1531. (c) Antipov, A. A.; Sukhorukov, G. B.; Leporatti, S.; Radtchenko, I. L.; Donath, E.; Möhwald, H. *Colloids Surf., A* **2002**, *198*, 535.
(3) (a) Stockton, W. B.; Rubner, M. F. *Macromolecules* **1997**, *30*, 2717. (b) Wang, L. Y.; Wang, Z. Q.; Zhang, X.; Shen, J. C.; Chi, L. F.; Fuchs, H. *Macromol. Rapid Commun.* **1997**, *18*, 509.
(4) Sukhishvili, S. A.; Granick, S. *Macromolecules* **2002**, *35*, 301.
(5) (a) Kaczmarek, H.; Szalla, A.; Kamiñska, A. *Polymer* **2001**, *42*, 6057. (b) Lau, C.; Mi, Y. *Polymer* **2002**, *43*, 823. (c) Jiang, M.; Li, M.; Xiang, M.; Zhou, H. *Adv. Polym. Sci.* **1999**, *146*, 121. (d) Tsuchida, E.; Abe, K. *Adv. Polym. Sci.* **1982**, 45.
(6) Zhang, Y.; Guan, Y.; Yang, S.; Xu, J.; Han, C. C. *Adv. Mater.* **2003**, *15*, 832.
(7) (a) Kozlovskaya, V.; Ok, S.; Sousa, A.; Libera, M.; Sukhishvili, S. A. *Macromolecules* **2003**, *36*, 8590. (b) Kharlampieva, E.; Sukhishvili, S. A. *Polym. Rev.* **2006**, *46*, 377. (c) Lee, D.; Rubner, M. F.; Cohen, R. E. *Chem. Mater.* **2005**, *17*, 1099.
(8) Singh, A.; Markowitz, M.; Chow, G. M. *Nanostruct. Mater.* **1995**, *5*, 141.
(9) (a) Huang, H.; Remsen, E. E.; Kowalewski, T.; Wooley, K. L. *J. Am. Chem. Soc.* **1999**, *121*, 3805. (b) Sanji, T.; Nakatsuka, Y.; Ohnishi, S.; Sakurai, H. *Macromolecules* **2000**, *33*, 8524. (c) Stewart, S.; Liu, G. *Chem. Mater.* **1999**, *11*, 1048.
(10) Emmerich, O.; Hugenberg, N.; Schmidt, M.; Sheiko, S. S.; Baumann, F.; Deubzer, B.; Weis, J.; Ebenhoch, J. *Adv. Mater.* **1999**, *11*, 1299.
(11) Landfester, K. *Adv. Mater.* **2001**, *13*, 765.

10.1021/cm070042n CCC: $37.00 
Published on Web 08/17/2007

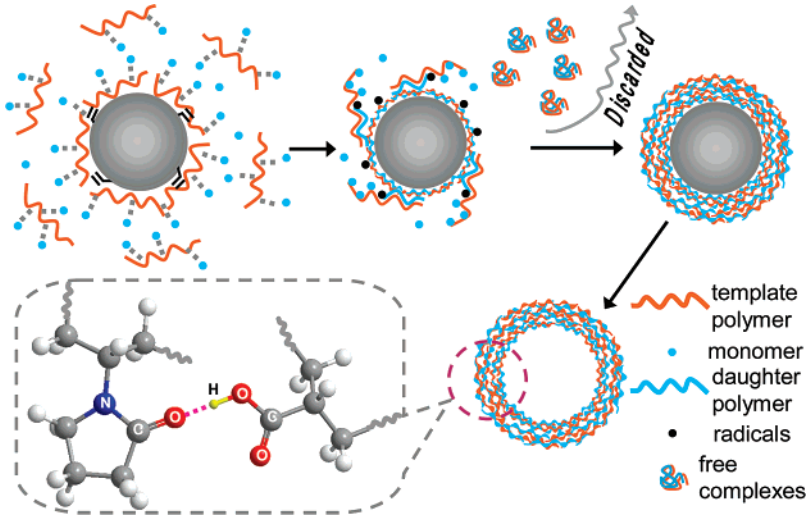


**Figure 1.** Schematic illustration to show the fabrication process of the hydrogen-bonded microcapsule by a template polymerization. (i) Initiation; (ii) "grafting from" to grow the shell; and (iii) core removal to produce the hollow capsule.

atomic transfer radical polymerization (ATRP),[13] have been adopted in different systems and for various purposes. The hollow capsules obtained from the emulsion polymerization and from the mini-emulsion polymerization are often of small size and of poor dispersion in water. Using dispersion polymerization, Fu et al. fabricated thermo-sensitive microcontainers,[1a] while Asher and Xu obtained hollow polystyrene capsules applicable in photonic crystals.[12]

Capsules fabricated by the methods mentioned previously are usually composed of only one component. However, hollow capsules composed of two or more components, such as the hydrogen-bonding system, often exhibit more tunable functions. The layer by layer (LBL) assembly on the sacrificing cores is such a technique, by which multiple components can be incorporated into the capsules. It has the merits of precise control over the capsule size, the shell thickness, and the composition.[14,15] However, when it is applied to the fabrication of the hydrogen-bonded microcapsules, the pH values of the solutions should be finely controlled to avoid aggregation of the building blocks and dissociation of the assembled layers.[7a]

Template polymerization is another useful method to obtain multicomponent materials.[16] In this technique, a polymer is used as the template to associate with monomers by hydrogen bonding, electrostatic force, or other interactions, followed by polymerization of the monomers in which propagation of a radical occurs along the template polymer chain during most of its lifetime. Radical template polymerization can yield polymer−polymer complexes held by cooperative interactions of complementary macromolecules.

Although template polymerization has been well-investigated, so far it has not been applied to forming an ultrathin layer on colloidal particles and further to fabricating hollow capsules except by our group.[17] In our previous work,[17] hollow polyelectrolyte microcapsules were fabricated by template polymerization driven by electrostatic interactions. However, fabrication of hollow capsules by template polymerization driven by hydrogen bonding still remains a challenge because of the decreased stability. Yet, the tunable features of this kind of microcapsule are more attractive.

In this work, the successful fabrication of hydrogen-bonded microcapsules by template polymerization will be demonstrated, exemplified by polymerization of acrylic acid (AA) in the presence of PVP molecules and colloidal silica particles that function as templates for polymer chain growth and capsule formation, respectively (Figure 1). The silica particles are first modified by 3-(trimethoxysilyl)propylmethacrylate to introduce C═C double bonds onto its surface. The added PVP can not only stabilize the particle suspension but also bind the AA monomers to form the PVP/AA conjugates. When the polymerization proceeds, the PVP/AA conjugates (the zip mechanism)[16a] are transformed into PVP/PAA complexes. Then, the initially adsorbed PVP/AA conjugates on the particle surfaces form the original shells, while those suspended PVP/AA conjugates form free complexes in the solution. As the polymerization proceeds, the shells become thicker and thicker mainly by the "grafting from" mechanism (i.e., a mechanism in which radicals in the shells initiate the polymerization of AA monomers conjugated with PVP) and also possibly by the "grafting to" mechanism (i.e., a mechanism in which the PVP/PAA complexes are grafted to the shells by radial coupling termination). Upon etching out the silica particle by the HF solution, hollow capsules composed of PVP and PAA complexes can be obtained.

(12) Xu, X.; Asher, S. A. *J. Am. Chem. Soc.* **2004**, *126*, 7940.
(13) (a) Mandal, T. K.; Fleming, M. S.; Walt, D. R. *Chem. Mater.* **2000**, *12*, 3481. (b) Duan, H.; Kuang, M.; Zhang, G.; Wang, D.; Kurth, D. G.; Möhwald, H. *Langmuir* **2005**, *21*, 11495.
(14) (a) Donath, E.; Sukhorukov, G. B.; Caruso, F.; Davis, S. A.; Möhwald, H. *Angew. Chem., Int. Ed.* **1998**, *37*, 2202. (b) Caruso, F.; Caruso, R. A.; Möhwald, H. *Science* **1998**, *282*, 1111. (c) Peyratout, C. S.; Dähne, L. *Angew. Chem., Int. Ed.* **2004**, *43*, 3762.
(15) (a) Caruso, F. *Chem.—Eur. J.* **2000**, *6*, 413. (b) Shi, X.; Briseno, A. L.; Sanedrin, R. J.; Zhou, F. M. *Macromolecules* **2003**, *36*, 4093.
(16) (a) Polowinski, S. *Prog. Polym. Sci.* **2002**, *27*, 537. (b) Szumilewicz, J. *Macromol. Symp.* **2000**, *161*, 183. (c) Polacco, G.; Cascone, M. G.; Petarca, L.; Maltinti, G.; Cristallini, C.; Barbani, N.; Lazzeri, L. *Polym. Int.* **1996**, *41*, 443.
(17) Feng, Z. Q.; Wang, Z.; Gao, C. Y.; Shen, J. C. *Mater. Lett.* **2006**, *61*, 2560.

Although template polymerization of acrylic acid in the presence of PVP has been well-investigated,[18] this is the first time hollow microcapsules have been fabricated by this technique. The resulting hollow capsules are formed with complexes originating from water soluble polymers by one step and show a good dispersion in water due to the stabilization effect of the template polymers.

## Experimental Procedures

**Materials.** Acrylic acid and potassium persulfate ($K_2S_2O_8$) were purified by distillation under reduced pressure and recrystallization in water, respectively. 3-(Trimethoxysilyl)propylmethacrylate (MPS), poly(ethylene glycol) diacrylate (PEGDA, $M_n = 258$) (Aldrich), PVP (30K), and rhodamine 6G (Rd6G, Aldrich) were used as received. Triply distilled water with a pH value of 5.5 was used in all the experiments.

**Microcapsule Fabrication.** The dried silica microparticles with a diameter of ~1 mm, prepared by the modified Stöber method,[19] were dispersed in 40 mL of anhydrous toluene, into which 2 mL of MPS was added. The mixture was stirred overnight, then centrifuged and washed sequentially with toluene and ethanol, each 3 times. The obtained MPS-modified microparticles were dried under reduced pressure.

To fabricate the core−shell particles, 1 g of MPS-grafted microparticles was dispersed in 50 mL of water under ultrasonication, into which 2.7 g of PVP and 0.03 g of $K_2S_2O_8$ were added. The amount of AA was varied from 0.5, to 0.2, to 0.1 mL. The final pH value of the reaction system turned out to be ~3. The polymerization was conducted in a $N_2$ atmosphere at 65 °C for 2 h under mechanical agitation at 400 rpm. After polymerization, these composite particles were collected by centrifugation and washed 3 times with triply distilled water. To obtain hollow microcapsules, a 0.4 mol/L HF solution was added to the composite particles, with a final HF concentration of 0.04 M. Ten minutes later, the mixture was centrifuged at 3000 rpm for 15 min (***Caution!*** *The HF solution is highly toxic and corrosive, and it should be handled with care in a fume cupboard.*). This process was repeated several times until the cores were completely removed. The resulting microcapsules were incubated in water with a pH value of 3.0. It would be demonstrated later that the microcapsules fabricated by this scheme were lightly cross-linked. These lightly cross-linked particles and capsules obtained from 0.5, 0.2, and 0.1 mL of AA were designated as LP-AA0.5, LP-AA0.2, and LP-AA0.1 and LC-AA0.5, LC-AA0.2, and LC-AA0.1, respectively. Here, L denotes lightly cross-linked, P denotes particles, and C denotes capsules.

To fabricate highly cross-linked microcapsules, 0.2 or 0.055 mL of PEGDA was added into the system, keeping the amount of AA constant (0.3 mL) and under the same reaction conditions. The resulting highly cross-linked particles and microcapsules were designated as HP-PEGDA0.2 and HP-PEGDA0.055 and HC-PEGDA0.2 and HC-PEGDA0.055, respectively. Here, H denotes highly cross-linked.

**Characterizations.** *Transmission Electron Microscopy (TEM).* For TEM analysis, samples were prepared by placing a drop of the particle or capsule suspensions onto copper grids and naturally drying. The pH values of the particle and capsule suspensions were 4.1 and 3.0, respectively. Copper grids coated with cellulose acetate films were used to support the microparticles and microcapsules. The samples were measured using TECNAL-10, Philips, and JEOL JEM-200CX instruments at an accelerating voltage of 100 kV.

*Scanning Electron Microscopy (SEM).* For SEM analysis, samples were prepared by placing a drop of the particle or capsule suspensions onto clean glass and naturally drying. The pH values of the particle and capsule suspensions were 4.1 and 3.0, respectively. After sputtering a thin gold layer, the samples were measured using SIRION-100 microscopy (RAITH) at an operation voltage of 3 keV.

*Atomic Force Microscopy (AFM).* The cross-linked microcapsules were dried naturally from triply distilled water on freshly cleaved mica. The topography of the microcapsules was observed using an AFM (Seiko Instruments SPI3800N) in dynamic force mode under ambient conditions.

*Confocal Laser Scanning Microscopy (CLSM).* The fluorescent images were captured using a confocal laser scanning microscope (Bio-Rad Radiance 2100) equipped with a 100× oil immersion objective. Equal volumes of capsule suspension and Rd6G solution (0.01 mg/mL) were mixed together. Rd6G could be adsorbed by microcapsule walls to render the microcapsules visible under CLSM. The excitation wavelength was set at 543 nm. Variable pH values were used to determine the capsule size.

*Elemental Analysis.* The microcapsules and complexes were dried from a suspension with a pH value of 4. Elemental analysis was carried out on a Flash EA 1112 instrument.

*FTIR Spectra*. The microcapsules were dried from a suspension with a pH value of 4. The dried microcapsules and PVP were ground with KBr powder, respectively. The mixtures were made into pellets under high pressure. FTIR spectra were recorded on a VETOR 22 spectrophotometer.

*ζ-Potential Measurement*. The ζ-potentials of the composite particles suspended in triply distilled water were measured by Zetasizer Nanoinstrument Nano Z equipment. Five parallel measurements were taken for each sample and averaged.

*Particle Size Measurement.* The intensity particle size distribution was determined by a Particle Size Analyzer (BI-90 Plus Brookhaven Instruments Co.). Ten parallel measurements were taken at pH 3 for each sample and averaged.

## Results and Discussion

**Microcapsule Fabrication.** The original (Figure 2a) and polymer coated silica particles (Figure 2b,c) were first characterized by SEM to compare their surface morphology changes. As can be seen in Figure 2b, the original smooth surfaces became rather rough after polymerization (LP-AA0.5), and some additional materials on the surfaces linked the dried particles together. By contrast, the surfaces of the highly cross-linked polymer covered particles (HP-PEGDA0.2) (Figure 2c) were as smooth as those of the control silica particles. The reasons for the rough surfaces of lightly cross-linked particles could be either the inhomogeneous polymerization on the silica particle surfaces or the uneven collapse of the shell layers as a result of drying. On the basis of the comparison between lightly and highly cross-linked particles, we can deduce that the latter reason should play a major role. The PAA/PVP complexes possess a relatively high mobility in the hydrated state and thus may reorganize their macroscopic structures due to the capillary force during drying. After the shell layers were highly cross-linked, however, both mobility and swelling ability of the shell layers

(18) (a) Muramatsu, R.; Shimidzu, T. *Bull. Chem. Soc. Jpn.* **1972**, *45*, 2528. (b) Tan, Y. Y. In *Comprehensive Polymer Science*; Allen, G., Bevington, J. C., Eds.; Pergamon Press: London, 1989; Vol. 3. p 245.
(19) (a) Stöber, W.; Fink, A. *J. Colloid Interface Sci.* **1968**, *26*, 62. (b) Bogush, G. H.; Tracy, M. A.; Zukoski, C. F. *J. Non-Cryst. Solids* **1988**, *95*, 104.

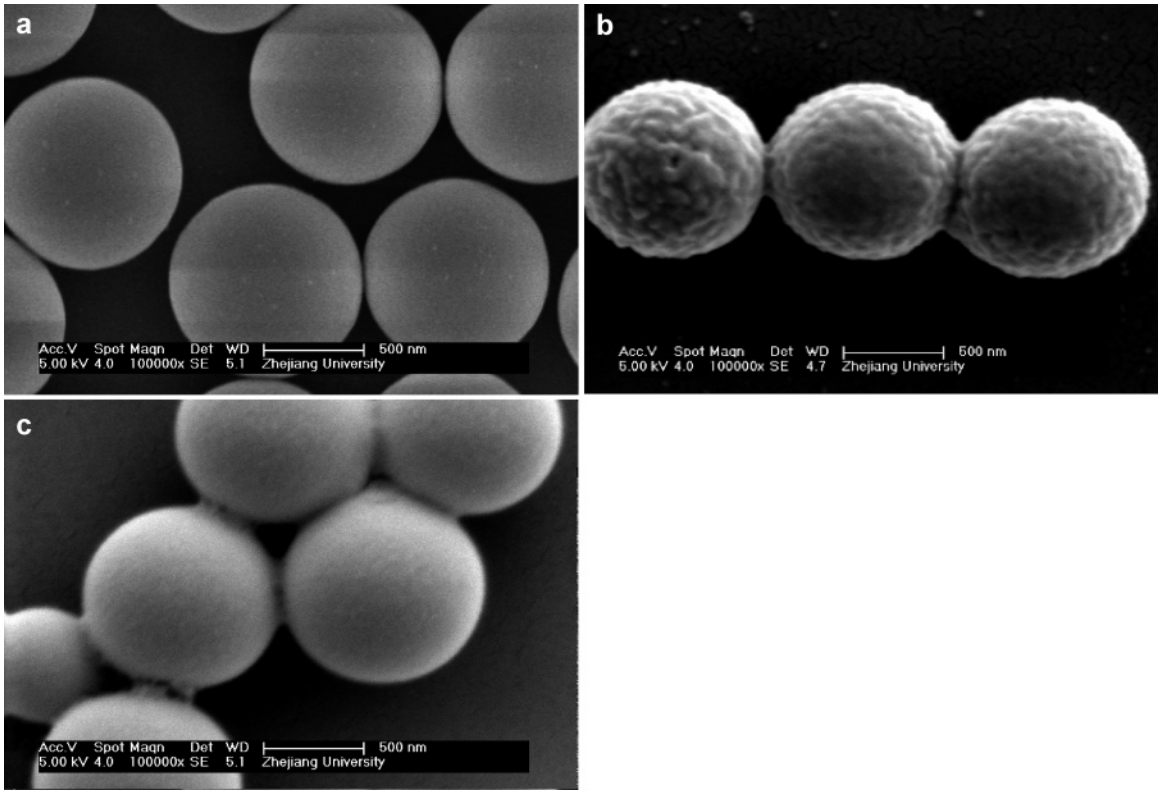


**Figure 2.** SEM images to show the surface morphologies of the silica particles before and after polymerization. (a) MPS-modified silica particles; (b) silica particles with lightly cross-linked polymer shells (LP-AA0.5); and (c) silica particles with highly cross-linked polymer shells (HP-PEGDA0.2).

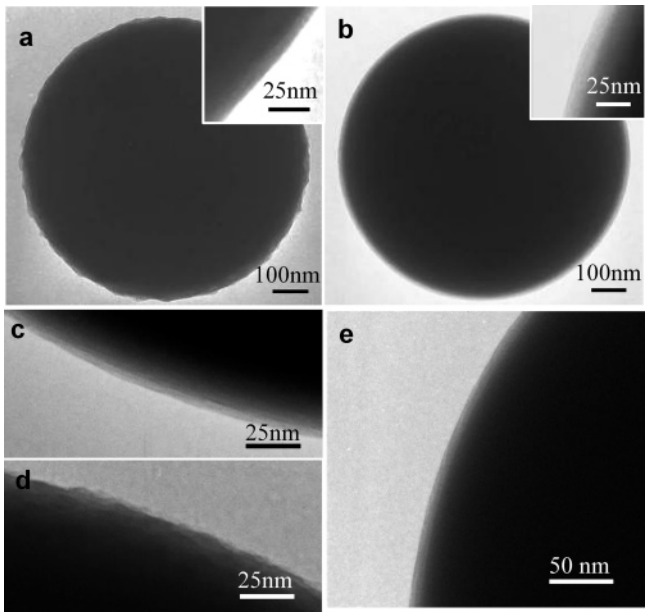


**Figure 3.** TEM images to show the silica particles with polymerized PAA/PVP shells. Panels a, c, and d are LP-AA0.5, LP-AA0.2, and LP-AA0.1, respectively, and panels b and e are HP-PEGDA0.2 and HP-PEGDA0.055, respectively. Insets of panels a and b are higher magnifications of the particle edges to show more clearly the polymer shells.

were significantly decreased, resulting in less reorganization upon drying and thus smoother surfaces.

To confirm the intactness of the shells, the composite particles were subjected to TEM characterization (Figure 3). Both lightly and highly cross-linked shells showed continuous structures on the silica particles. Again, the highly cross-linked shells (Figure 3b,e) were more homogeneous than the lightly cross-linked shells (Figure 3a,c,d). From the enlarged images of the composite particles, the thickness of the lightly cross-linked shells of LP-AA0.5 (Figure 3a, inset) was estimated to be ~10 nm. When the monomer volume was decreased to 0.2 mL (LP-AA0.2), the shell thickness of the lightly cross-linked particles decreased to 5 nm (Figure 3c). For LP-AA0.1, the shells could not fully cover the whole particles (Figure 3d), from which no capsules were derived after core removal. When the cross-linker PEGDA was added, the shell thickness increased slightly in comparison to the lightly cross-linked counterpart with the same total monomer volume, for example, HP-PEGDA0.2 had a shell thickness of ~13 nm (Figure 3b, inset). At a lower cross-linker concentration, intact shells could be formed on the particle surfaces with thinner shells, for example, ~8 nm for HP-PEGDA0.055.

Hollow microcapsules were obtained upon removal of the silica templates by HF etching. From the TEM images (Figure 4a,b), one can find that the silica cores had been removed completely since all the microcapsules (LC-AA0.5 and HC-PEGDA0.2) were collapsed. As can be seen more clearly in the SEM images (Figure 4c,d), both kinds of microcapsules exhibited folds and creases that were typical for the capsules with ultrathin shells. Being analyzed more in detail, the highly cross-linked capsules (HC-PEGDA0.2) displayed clear creases in the SEM image, whereas the lightly cross-linked microcapsules (LC-AA0.5 and LP-AA0.2) showed a relatively flat morphology. This gives us a hint that the highly cross-linked microcapsules possess a higher rigidity.[20]

(20) Tong, W. J.; Gao, C. Y.; Möhwald, H. *Chem. Mater.* **2005**, *17*, 4610.

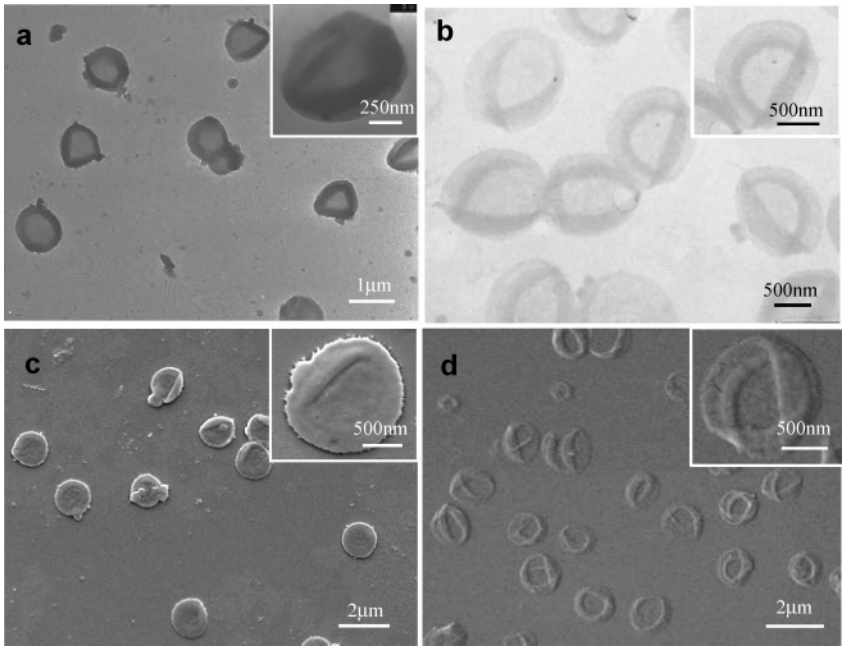


**Figure 4.** TEM (a and b) and SEM (c and d) images of hollow microcapsules. (a and c) LC-AA0.5 and (b and d) HC-PEGDA0.2.

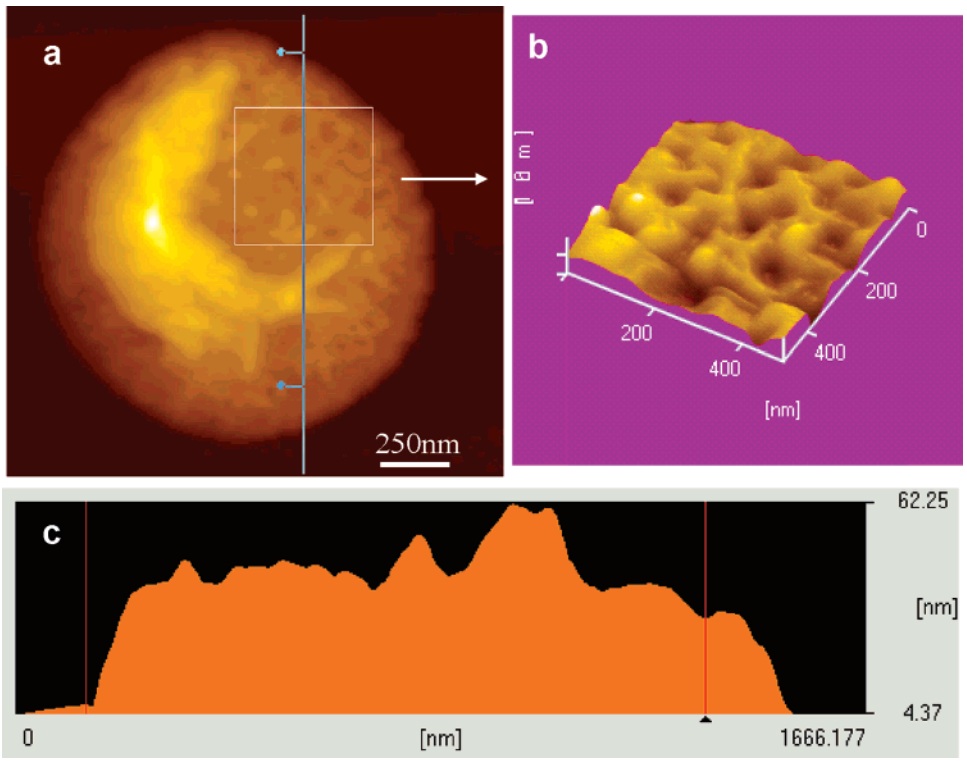


**Figure 5.** (a) AFM image of the highly cross-linked PAA/PVP microcapsule (HC-PEGDA0.2). (b) Higher magnification of panel a in the flat region marked by the rectangular box in panel a. (c) Line profile of the capsule in the region shown by the line in panel a.

To investigate the microstructures of the highly cross-linked capsules, the highly cross-linked hollow capsules (HC-PEGDA0.2) were further subjected to AFM(Figure 5). The folds and creases were also visible. The thickness of the double shells was estimated to be 26 nm, corresponding to a shell thickness of 13 nm that was in accord with the TEM results (Figure 3b). The enlarged image shown in the inset of Figure 5 reveals that the surface of the microcapsule was not smooth on a nanometer scale. This is not contradictory to the results of Figures 2 and 3, which were obtained on a micrometer scale and with the existence of the silica particles. The rough surface was also typical for the capsules with ultrathin shells, which resulted from the segregation of the complexes on a nanometer scale during drying.[21] Of course, in this particular case, one cannot fully exclude the possibility of inhomogeneous polymerization on the particle surfaces.

The complexation between PVP and PAA via hydrogen bonding was confirmed by the shift of the carbonyl absorption bands of PAA and PVP in the FTIR spectra (Figure 6).

(21) (a) Leporatti, S.; Voigt, A.; Mitlöhner, R.; Sukhorukov, G.; Donath, E.; Möhwald, H. *Langmuir* **2000**, *16*, 4059. (b) Gao, C. Y.; Leporatti, S.; Donath, E.; Möhwald, H. *J. Phys. Chem. B* **2000**, *104*, 7144.

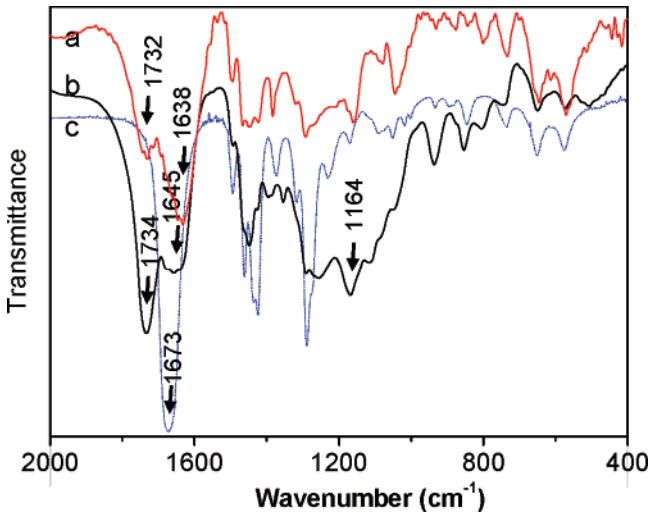


**Figure 6.** FTIR spectra of (a) lightly cross-linked (LC-AA0.5) and (b) highly cross-linked (HC-PEGDA0.2) microcapsules.

The carbonyl absorption bond of PVP in the microcapsules shifted from 1673 to 1638 $cm^{-1}$, as is consistent with previous literature.[22,23] The peak at 1712 $cm^{-1}$ is assigned to the carboxylic groups of PAA in an intramolecular hydrogen-bonding state.[22] When the carboxylic groups complexed with PVP, the absorption band shifted to 1732 $cm^{-1}$.[23] Comparing the FTIR results of the HC-PEGDA0.2 and LC-AA0.5 microcapsules, one can find that the relative intensities of the carbonyl vibrations in PAA and PVP had been changed, indicating the variance of the capsule structures. In the case of highly cross-linked microcapsules, the intensity of the strong overlapping band (1734 $cm^{-1}$) of the carbonyl groups of the cross-linkers and PAA suppressed the intensity of the carbonyl groups of PVP. Moreover, the asymmetric stretching vibration of C−O−C (1164 $cm^{-1}$) of the ester groups confirmed the presence of the cross-linkers. All these results demonstrated that the capsules are indeed composed of hydrogen-bonded PVP and PAA.

**Shell Formation Mechanism and Capsule Compositions.** The shell formation dynamics and capsule compositions are crucial for exploring the mechanism for shell formation. First, to reveal the shell formation dynamics, the dependency of shell thickness on the polymerization time was investigated. The MPS-modified silica particles were incubated in the PVP or PVA/AA solution (corresponding to conditions of LP-AA0.5) for 20 min and were washed using the same procedures for the capsule fabrication. Figure 7a shows that the particle surfaces were loosely covered by PVP molecules, which should be mainly driven by hydrophobic forces. When AA monomers were further introduced, many droplet-like hemispheres were observed on the particle surfaces (Figure 7b), which indicated that PVP or PVP/AA can be rather stably adsorbed onto the MPS-modified silica particles in solution. The droplet-like structures were formed due to a typical dewetting process during drying, thus implying a stronger hydrophilicity of the PVP/AA component. After polymerization for 5 min, complete shells with a thickness of 4.5 nm were formed on the silica particles (Figure 7c), which were strong enough to yield intact hollow capsules after etching off the silica particles. This implied that the PVP bound AA monomers on the silica particle surfaces polymerized very quickly due to the template effect, yielding thin shells during a very short period. As the polymerization went on, the shell thickness increased almost linearly to 5.2 nm (Figure 7d, 10 min), 6.0 nm (Figure 7e, 20 min), 7.1 nm (Figure 7f, 30 min), 8.6 nm (Figure 7g, 1 h), and 13.4 nm (Figure 7h, 3 h). It was revealed by elemental analysis that the molar ratios of AA/VP for all the derived capsules were almost equal to 1. This implied that PVP and PAA were equally immobilized onto the originally formed shells. Moreover, DLS detected that the average size of free PVP/PAA complexes formed during the polymerization at pH 3 is as large as 650 nm. Together with the fact that the shell surfaces remained smooth during all the polymerization times, with no sign of apparent tiny particles on the shells, we can conclude here that the shells were most possibly formed by a "grafting from" mechanism.

In the next experiment, the AA amount and polymerization time were controlled as 0.3 mL and 2 h, respectively, while the PVP amount was varied. Figure 8 shows that the shell thickness decreased from 12 to 6.8 nm when the PVP amount increased from 1.6 to 3.7 g. It was revealed again by elemental analysis that the molar ratios of AA/VP for all the derived capsules were almost equal to 1 (a detailed discussion can be found later). At a higher PVP concentration, the average amount of associated AA per PVP molecule and the amount of free AA monomers decreased. If the initially adsorbed PVP amount remained unchanged, the growth rate of the shells would decrease because it takes a longer time to attract other AA molecules to associate with the initially adsorbed PVP, which was insufficiently conjugated. Taking into account the results of Figures 7 and 8, it can be deduced that the "grafting to" mechanism mentioned previously plays a minor role in shell formation. In this case, the collision probability between the particles and the PVP/PAA complexes would be less influenced because the total amount of PVP/PAA complexes was decided by the PAA content despite that PVP was stoichemically excessive.

In principle, the MPS-modified silica particles can also be grafted with a layer of PAA, which can then complex with the PVP molecules by hydrogen bonding to form denser shells. To clarify whether this mechanism works in our system, polymerization of AA was conducted under the same conditions of LP-AA0.5 except that PVP was not added. Figure 9a shows that stable PAA layers were actually formed on the silica particle surfaces, with a thickness of ~2.1 nm. These particles dispersed better in water than the MPS-modified ones, demonstrating the more hydrophilic nature of the PAA-grafted particles. Next, these PAA-grafted particles were suspended in a 2 mg/mL PVP solution with a pH value of 3.5 for 20 min and were washed with water at pH 3.5 3 times. After the adsorption of PVP, the layer thickness increased to 4 nm (Figure 9b). After core removal, these particles could hardly produce intact capsules as the LC-AA0.5. These phenomena demonstrate that the grafted PAA can surely conjugate with PVP molecules driven by

(22) Baranovsky, V. Y.; Kotlyarsky, I. V.; Etlis, V. S.; Kavanov, V. A. *Eur. Polym. J.* **1992**, *28*, 1427.
(23) Chun, M. K.; Cho, C. S.; Choi, H. K. *J. Controlled Release* **2002**, *81*, 327.

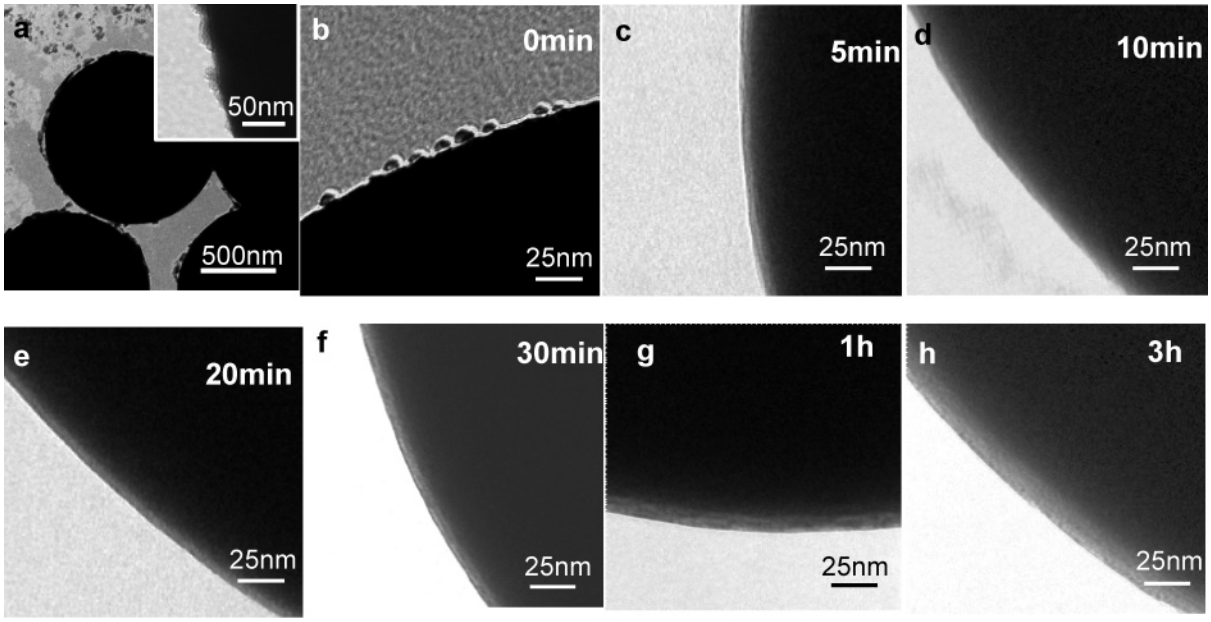


**Figure 7.** TEM images of silicon particles after incubation in (a) PVP solution (2.7 g of PVP in 50 mL of water, pH 3) or (b) in PVP/AA solution (2.7 g of PVP and 0.5 mL of AA in 50 mL of water, pH 3) for 20 min, followed by sufficient rinsing using the same conditions of LP-AA0.5. TEM images of the core−shell silicon particles obtained at different polymerization times are shown in the corresponding images (c−h). Shell thicknesses: (c) 4.5 nm, (d) 5.2 nm, (e) 6.0 nm, (f) 7.1 nm, (g) 8.6 nm, and (h) 13.4 nm.

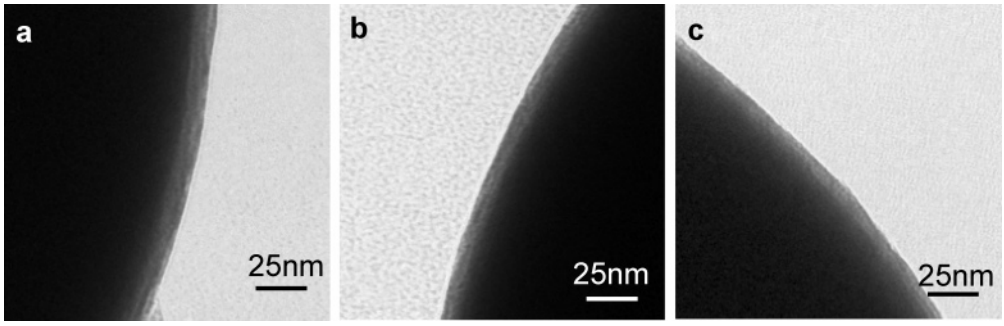


**Figure 8.** TEM images of the core−shell particles prepared at different PVP concentrations. Polymerization conditions were 0.3 mL of AA and 0.03 g of KPS at 65 °C for 2 h, with (a) 1.6 g of PVP, (b) 2.7 g of PVP, and (c) 3.6 g of PVP. Shell thicknesses: (a) 12 nm, (b) 8.25 nm, and (c) 6.8 nm.

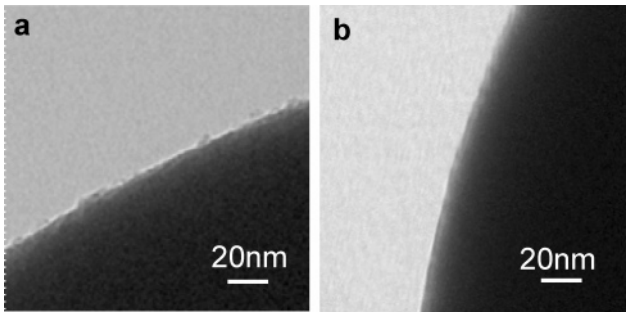


**Figure 9.** TEM images of (a) PAA-grafted particles and (b) the particles in panel a after incubation in 2 mg/mL PVP solution for 20 min at pH 3, followed by sufficient rinsing. Polymerization conditions for the PAA-grafted particles were the same as that of UP-AA0.5 except for the absence of PVP.

the hydrogen bonding. However, the layer thickness was much smaller than that of LP-AA0.5 obtained by template polymerization. Therefore, the grafting and sequential conjugating mechanism can be safely excluded.

Here, the C═C double bonds on the silica particles are indispensable, through which the PAA/PVP complexes are covalently immobilized onto the particle surfaces. To demonstrate the importance of this surface modification, we conducted the following comparison experiments. First, bare silica particles were used. We found that severe aggregation occurred during the polymerization, implying that the hydrophilic particles were hardly protected by the PVP molecules, especially in the presence of PAA. Second, the particle surfaces were modified with phenyltrimethoxysilane to endow the particles with enough hydrophobicity. This time, aggregation during polymerization was avoided, but severe aggregation appeared after centrifugation. After core removal, we could hardly find mono-dispersed capsules. Many broken pieces instead of intact capsules were observed. In both cases, we believe that the PVP or PVP/AA complexes can also be adsorbed onto the silica particle surfaces initially. However, along with the proceeding of the polymerization, the formed PVP/PAA complexes tended to be desorbed from the particle surfaces because of the lack of enough binding strength. All these results demonstrated that stable linkages between the particle surfaces and the PAA/PVP complexes could be achieved by modification of the silica particles with the C═C groups, while the hydrophobicity played a relatively minor role.

To determine the quantities of PAA and PVP in the capsules, the hollow capsules were subjected to elemental analysis (Table 1). According to the contents of nitrogen and

**Table 1. Elemental Analysis Results of Various PAA/PVP Microcapsules[a]**

| | element content | | | polymer content | | molar ratio |
|---|---|---|---|---|---|---|
| | N (wt %) | C (wt %) | H (wt %) | PAA (wt %) | PVP (wt %) | AA/VP |
| LC-AA0.5 | 6.45 | 52.15 | 7.44 | 38.3 | 50.8 | 1.14 |
| LC-AA0.5* | 7.15 | 53.56 | 7.43 | 33.58 | 56.69 | 0.97 |
| HC-PEGDA0.055 | 6.41 | 56.73 | 7.40 | | 50.8 | |
| HC-PEGDA0.055* | 6.61 | 56.22 | 7.38 | | 52.4 | |
| LC-AA0.3 | 7.35 | 54.97 | 7.05 | 34.34 | 58.28 | 0.908 |
| LC-AA0.2 | 6.76 | 53.64 | 7.45 | 38 | 53.6 | 1.09 |
| HC-PEGDA0.2 | 2.68 | 54.00 | 6.98 | | 21.2 | |

[a] LC-AA0.5* and HC-PEGDA0.055* denote, respectively, LC-AA0.5 and HC-PEGDA0.055 after they were incubated in a pH 11 solution for 1 day and dried in a pH 4 solution.

carbon, taking LC-AA0.5, for example, the weight percentages of PAA and PVP were calculated as 38.3 and 50.8%, respectively, corresponding to a molar ratio of [COOH]/[C═O] of 1.14. The results of other samples are summarized in Table 1, from which one could find that all the molar ratios of [COOH]/[C═O] are roughly close to 1. The equibase molar (stoichiometric) composition in these samples was consistent with previous literature,[24] which confirmed the template polymerization mechanism. Because of the existence of the cross-linkers (PEGDA), the PAA content in the microcapsules with the addition of cross-linkers could not be derived from the elemental analysis data. The lower N content of HC-PEGDA0.2 (2.68%) than that of the LC-AA0.5 (6.45%) indicated the huge contribution of the cross-linker (PEGDA) to the capsule mass, while the same N content of HC-PEGDA0.055 (6.41%) as that of the lightly cross-linked microcapsules was consistent with the smaller feeding of PEGDA (∼10 wt % of the total mass). The ζ-potential recorded negative values for both the lightly cross-linked (LP-AA0.5) ($-35.2 \pm 0.47$ mV) and the highly cross-linked (HP-PEGDA0.2) ($-36.5 \pm 2.23$ mV) particles in triply distilled water, which demonstrated the existence of carboxylic groups in the shells.

An important factor determining the template polymerization is the similarity of the molecular weight of the daughter polymers to that of the template polymers. In our case, however, it is impossible to separate the daughter polymers because of the grafting of PAA to PVP, a phenomenon that has also been observed by Al-Alawi and Saeed when they conducted the template polymerization of AA in the presence of PVP.[25] To demonstrate the strong interaction between PAA and PVP molecules, LC-AA0.5 and HC-PEGDA0.055 were incubated in alkaline solution with a pH value of 11 for 1 day, followed by sufficiently washing with water at pH 11. Surprisingly, both kinds of capsules could survive the treatment. Elemental analysis revealed that the AA/VP ratios of both kinds of microcapsules remained unchanged (Table 1). These results demonstrated the strong interactions, most possibly the covalent bonding, between PAA and PVP molecules, otherwise PVP would be removed in alkali solution.[26] The grafting of PAA to PVP may occur during polymerization as a result of the chain transfer reaction. Moreover, free radicals can also be generated on the PVP chains,[25] thereby initiating the graft polymerization.

**Table 2. Elemental Analysis Results of Various PAA/PVP Complexes[a]**

| | element content | | | polymer content | | molar ratio |
|---|---|---|---|---|---|---|
| | N (wt %) | C (wt %) | H (wt %) | PAA (wt %) | PVP (wt %) | AA/VP |
| LCom-AA0.5 | 7.38 | 56.56 | 7.41 | 37.2 | 58.5 | 0.98 |
| LCom-AA0.5# | 7.75 | 57.39 | 7.60 | 35.2 | 61.4 | 1.01 |
| LCom-AA0.5#S | 6.39 | 50.20 | 7.20 | PAA-Na 46.9 | 50.35 | 1.08 |
| Com-PVP/PAA | 6.45 | 55.28 | 7.17 | 44.12 | 51.22 | 1.33 |
| Com-PVP/PAA-S | 0.17 | 35.52 | 4.51 | PAA-Na 90.5 | 1.35 | 79.16 |

[a] LCom-AA0.5 and LCom-AA0.5# denote the PVP/PAA complexes formed under the same conditions as LC-AA0.5 with and without the silica particles, respectively. LCom-AA0.5#S denotes the residue after LCom-AA0.5# was treated with a separation process. Briefly, LCom-AA0.5# was incubated in NaOH solution at pH 9 for 10 min and was then dropped into a large amount of absolute ethanol under agitation. Precipitates were collected by centrifugation and were treated with 1 M NaOH solution again. After the same precipitation process, the final residue was analyzed. Com-PVP/PAA denotes PVP/PAA complexes that were obtained by blending both polymers at pH 2 and purified by centrifugation. Com-PVP/PAA-S denotes the residue after Com-PVP/PAA was treated with a separation process like that of LCom-AA0.5#S.

We further analyzed the PVP/PAA complexes formed during the polymerization (Table 2). Results showed that LCom-AA0.5 and LCom-AA0.5# had the same AA/VP ratios of ∼1, although the former was prepared with the existence of silica particles, while the was latter not, and that no changes occurred in the composition of LCom-AA0.5# before and after a separation process. In a control experiment, however, the blend of PVP and PAA (Com-PVP/PAA) could be easily separated to give a very high ratio of PAA to PVP in the final product (Com-PVP/PAA-S in Table 2). This reveals two facts: (1) no strong interactions exist between PAA and PVP in alkaline solution and (2) the separation is valid to separate the physical blend of PAA and PVP.

On the basis of all the previous results, the mechanism for the shell formation on the MPS-modified particles can be proposed. The MPS modification endows the particles with hydrophobicity and reactivity. PVP plays two roles here. One is to serve as the template polymer, which can bind the AA monomers and guide their alignment via hydrogen bonding between the carbonyl −(−C═O) and carboxyl (−COOH) groups (Figure 1, left). The other role is to serve as a stabilizer. Because the amount of PVP here is stoichiometrically larger than that of PAA, the excess PVP can stabilize the formed PAA/PVP complexes, besides stabilizing the silica particles. Actually, the severe aggregation of complexes will appear if the amount of PVP is not enough. In this solution, the PVP/AA conjugates can be adsorbed onto the particle surfaces, which will rapidly form thin shells on the particle surfaces upon initiation (Figure 1, middle). As the polymerization proceeds, the shell thickness increases steadily by a "grafting from" mechanism mentioned previously (Figure 1, right). As a result, the final shells are formed, with an equal ratio of AA to VP.

(24) (a) Bimendina, L. A.; Roganov, V. V.; Bekturov, E. A. *Organized Structures in Polymer Solutions and Gels*; Wiley Interscience: New York, 1974; p 65. (b) Ferguson, J.; McLeod, C. *Eur. Polym. J.* **1974**, *10*, 1083.
(25) Alawi, S.; Saeed, N. A. *Macromolecules* **1990**, *23*, 4474.
(26) (a) Kozlovskaya, V.; Kharlampieva, E.; Mansfield, M. L.; Sukhishvili, S. A. *Chem. Mater.* **2006**, *18*, 328. (b) Kozlovskaya, V.; Sukhishvili, S. A. *Macromolecules* **2006**, *39*, 6191. (c) Kozlovskaya, V.; Sukhishvili, S. A. *Macromolecules* **2006**, *39*, 5569.

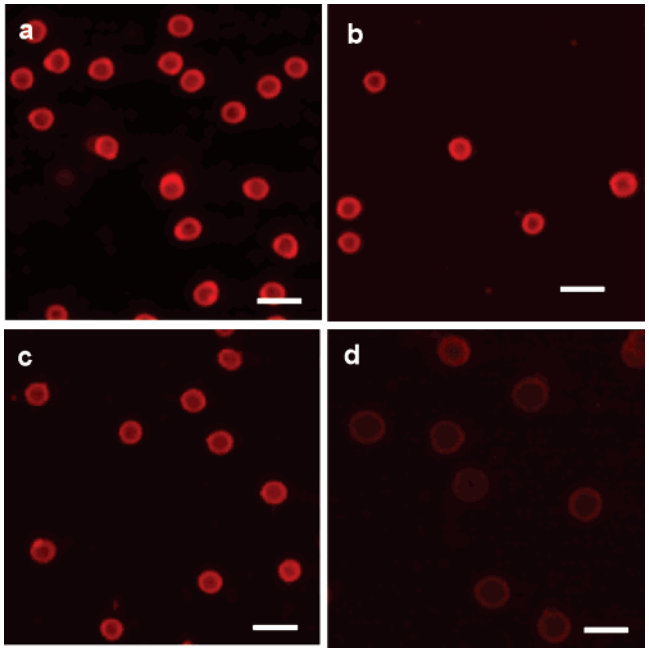


**Figure 10.** CLSM images of different capsules suspended in solutions of different pH values. Panels a−c are LC-AA0.5, LC-AA0.2, and HC-PEGDA0.2 in water with a pH value of 1.5, respectively. (d) Same capsules of panel c suspended in pH 13 solution. Microcapsules were stained with rhodamine 6G for observation. Scale bar is 2 $\mu$m.

**Stimuli-Responsiveness of Microcapsules.** The as-prepared microcapsules exhibited very good dispersion in water as shown in Figure 10. All the microcapsules, regardless of additional cross-linking, had a round-shaped morphology with neglectable aggregation. Therefore, it is convenient to further mediate the microcapsule properties such as pH-responsiveness because the hydrogen bonding is intrinsically controlled by the bulk pH value.

As compared to the microcapsules at low pH values (Figure 10c), the capsule size apparently increased in high pH solution (Figure 10d). This can be understood as a result of the loss of hydrogen bonding and the charge repulsion between the deprotonated -$COO^-$ groups, as has been previously observed in the case of polyelectrolyte multilayer microcapsules.[27] To elaborate more details of the pH-mediated capsule swelling behavior, here the HC-PEGDA0.055 and LC-AA0.5 microcapsules were subjected to different pHs. As shown in Figure 11, diameters of both capsules increased along with the pH increase, following a sigmoidal regime. The sharpest changes took place in the pH regions from 4.3 to 5.3 for LC-AA0.5 and from 5.5 to 7 for HC-PEGDA0.055, respectively. The transition point at pH 4.7 for LC-AA0.5 matched well with the p$K_a$ value (4.6) of PAA,[28] which was consistent with previous results.[29] However, as compared to the huge swelling degree of LC-AA0.5, the swelling degree of HC-PEGDA0.055 was only half that of LC-AA0.5. Moreover, the transition point of HC-PEGDA0.055 shifted to a higher pH value as well. It is

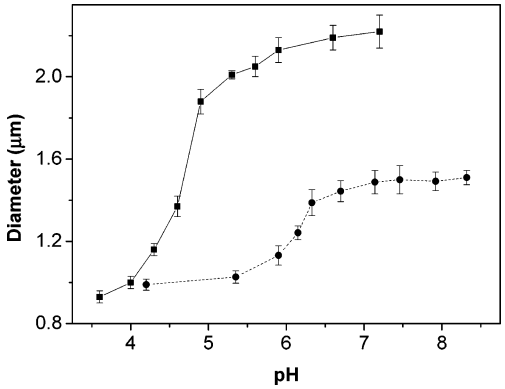


**Figure 11.** Variation of diameters of highly cross-linked capsules (circles, HC-PEGDA0.055) and lightly cross-linked capsules (squares, LC-AA0.5) as a function of pH value. Diameters of the capsules were measured under CLSM. pH value was tuned by 0.01 M phosphate buffer.

understandable that the capsule swelling behavior depends on the interplay of charge repulsion strength and cross-linking degree. At low pH values, the carboxylic groups are in a state of protonation and form hydrogen bonds with the carbonyl groups to hold the initial capsule structure. At high pH values, deprotonation of the carboxylic groups takes place, thus leading to the breakage of hydrogen bonding and repulsion between the PAA chains. In the case of a low degree of cross-linking such as LC-AA0.5, huge swelling occurred, with little influence on the apparent p$K_a$ value. However, in the case of a high degree of cross-linking such as HC-PEGDA0.055, the swelling was suppressed by the cross-linking points, leading to a difficulty of swelling that resulted in low degree of swelling and the shift of the transition point to high pH values. Since the hydrogen bonding between PEG and PAA can be destroyed at rather low pH values (3.6),[4] the contribution of the PEG segments in HC-PEGDA0.055 to the shift of the transition point can be neglected. To illustrate the reversible swelling−shrinking process tuned by the pH change, the swollen microcapsules were incubated in water at pH 1.2 again. As shown in Figure 12, both kinds of microcapsules could reversibly swell and shrink at high and low pH values, respectively. For LC-AA0.5 (Figure 12a−d), their diameters increased from 1 to 2.9 $\mu$m when the pH of the solution was changed from 1.5 to 12. Interestingly, a subsequent incubation in water at pH 1.2 caused irregular shrinking of the swollen capsules (Figure 12c), implying that the initial stretching force on the capsule walls had resulted in slippage between adjacent chains, namely, plastic deformation. In the case of HC-PEGDA0.055 (Figure 12 e−h), the capsules increased their diameters from 1 to 1.8 $\mu$m when the pH value was changed from 1.5 to 12 and then recovered their sizes completely when the pH value was decreased to 1.2. No sign of plastic deformation was observed. This swelling−shrinking process could be easily controlled by the bulk pH and could be repeated at least for several circles. Therefore, the additional cross-linking can greatly enhance the stability of the microcapsules against large pH fluctuations, thereby making the resulting microcapsules more applicable for practical applications, such as drug loading and release.[30]

(27) Biesheuvel, P. M.; Mauser, T.; Sukhorukov, G. B.; Möhwald, H. *Macromolecules* **2006**, *39*, 8480.
(28) Li, X.; Wu, W.; Wang, J.; Duan, Y. *Carbohydr. Polym.* **2006**, *66*, 473.
(29) (a) Elsner, N.; Kozlovskaya, V.; Sukhishvili, S. A.; Fery, A. *Soft Matter* **2006**, *2*, 966. (b) Oyama, H. T.; Hemker, D. J.; Frank, C. W. *Macromolecules* **1989**, *22*, 1255.
(30) Gao, C. Y.; Möhwald, H.; Shen, J. C. *Chem. Phys. Chem.* **2004**, *5*, 116.

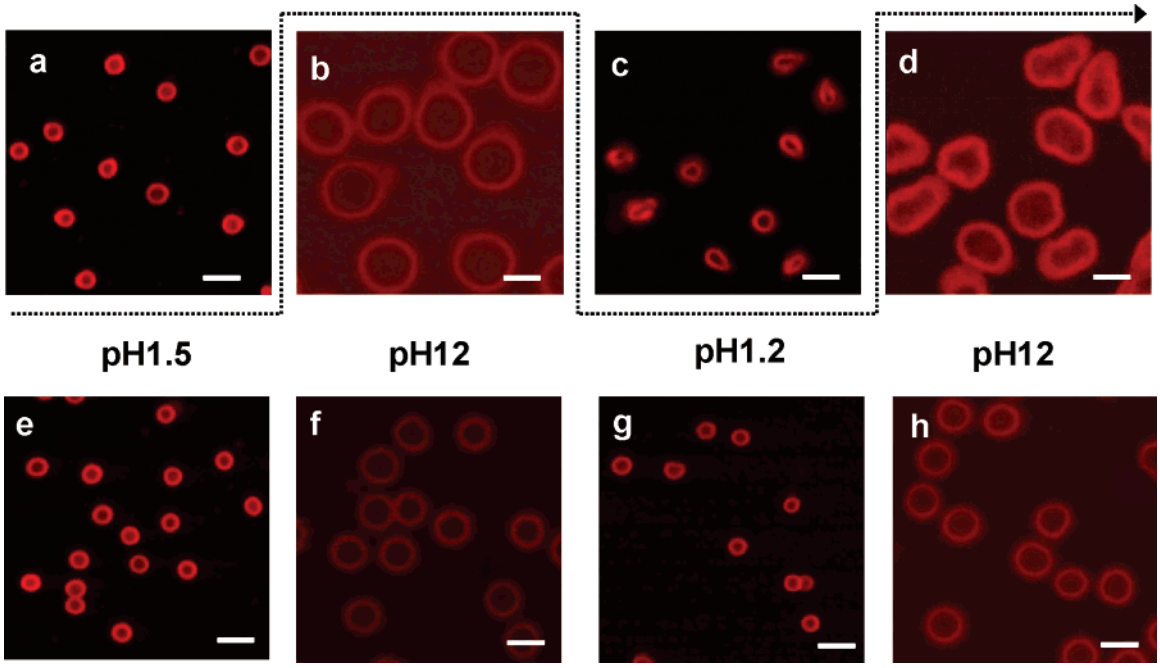


**Figure 12.** CLSM images to show the reversible swelling−deswelling of LC-AA0.5 (a−d) and HC-PEGDA0.055 (e and f) in response to the pH value of bulk solution. Scale bar is 2 $\mu$m.

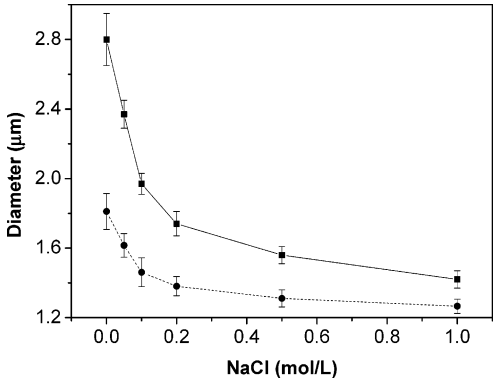


**Figure 13.** Variation of diameters of lightly cross-linked capsules (squares, LC-AA0.5) and highly cross-linked capsules (circles, HC-PEGDA0.055) as a function of NaCl concentration at pH 11.

It is well-known that the charge repulsion can be effectively screened by salt.[26a,31] In our case, the swollen microcapsules at pH 11 shrunk gradually along with the increase of the NaCl concentration in the bulk solution (Figure 13). In 1 M NaCl, both kinds of capsules almost recovered their initial sizes of low pH, implying that the charge repulsion between the PAA chains is almost screened by the salt.

## Conclusion

Herein, we reported the fabrication hollow hydrogen-bonded PVP/PAA microcapsules based on template polymerization. In a solution containing the MPS-modified silica particles and PVP molecules, polymerization of AA results in continuous shell layers on the silica particle surfaces. Here, both the PVP molecules and the silica particles function as templates to guide the alignment of AA monomers and to support the immobilization of the PVP/PAA complexes, respectively. After sacrificing the cores, hollow microcapsules with a shell thickness of 4 to ~13 nm were obtained. Their hollow nature was confirmed by TEM, SEM, AFM, and CLSM. The hydrogen bonding between PVP and PAA in the microcapsules, which is the basis of the template polymerization and the formation of microcapsules, was confirmed by FTIR spectroscopy. The chemical composition of the microcapsules was estimated by elemental analysis. Characterizations demonstrate that there exist strong interactions between PAA and PVP molecules, most possibly the covalent grafting of PAA to PVP. The microcapsules increased their sizes along with the increase of pH, following a sigmoidal regime. The swelling−deswelling process of the microcapsules is completely reversible at high and low pH values, which provides a convenient way to mediate the capsule properties. The added cross-linkers are helpful to obtain microcapsules with a higher stability against large pH fluctuations. Therefore, this work broadens the capsule fabrication techniques and enriches the capsule family, which has important applications and is under extensive study now.

**Acknowledgment.** This study was financially supported by the Natural Science Foundation of China (20434030), the Major State Basic Research Program of China (2005CB623902), and the National Science Fund for Distinguished Young Scholars of China (50425311).

CM070042N

(31) Ibarz, G.; Dähne, L.; Donath, E.; Möhwald, H. *Adv. Mater.* **2001**, *13*, 1324.